Effect of Brine Salinity on the Stability of Hydrate-in-Oil Dispersions and Water-in-Oil Emulsions

Zachary M. Aman, Agnes Haber, Nicholas Ling,*

Alexandra Thornton, Michael L. Johns, Eric F. May

Centre for Energy, School of Mechanical and Chemical Engineering,

University of Western Australia, 35 Stirling Highway, Crawley, WA 6009, AUSTRALIA

The stability of hydrate-in-oil dispersions is a critical parameter in assessing the risk of flowline blockage due to particle aggregation or wall deposition. Many studies of hydrate particle transportability have used deionized water to form the dispersion; however, the resulting lack of ions means that the crude oil's natural surfactants will be less active, which does not represent production conditions. This study presents a new investigation of both hydrate-in-oil dispersion stability and water-in-oil emulsion stability, measured with a differential scanning calorimeter (DSC) and low-field nuclear magnetic resonance (NMR) apparatus, respectively. The results show that hydrate-in-oil dispersion stability increases directly with sodium chloride (NaCl) mass fraction in the aqueous phase; above 5 wt% NaCl, the dispersion was observed to be stable over ten hydrate formation-dissociation trials. This was comparable with the dispersion stability observed previously when an ionic surfactant was dosed at 2 wt% into the same crude oil. In contrast, only 0.1 wt% NaCl was required to stabilize water-in-oil emulsions over a four day observation period. This comparison suggests that, for crude oils containing natural surfactants, the risk of hydrate blockage may decrease as brine salinity increases from 1 to 10 wt%, without affecting the stability of the water-in-oil emulsion. The results demonstrate that experimental studies on hydrate- or water-in-crude oil systems should be performed with realistic values of brine salinity, to accurately capture dispersion stability.

Keywords: *gas hydrate, emulsion stability, surfactant adsorption, flow assurance*

Corresponding author (Zachary M. Aman). zachary.aman@uwa.edu.au, +61 8 6488 3078

1 INTRODUCTION

Gas hydrates are crystalline inclusion compounds, where molecular water cages enclathrate light hydrocarbon species (e.g. methane) at high-pressure and low temperature conditions.[1] Hydrate formation represents a critical risk in subsea oil and gas pipelines; fluids exit the wellbore under high pressure and cool as the pipeline used to transport them is often exposed to cool seawater. In severe cases, hydrates may completely occlude the flowline, requiring costly remediation techniques that introduce operational and safety hazards.[2] The following four-step process of hydrate plug formation was hypothesized by Turner et al.[3] in collaboration with J. Abrahamson for oil-continuous systems: (i) emulsification of water droplets in the liquid hydrocarbon phase;[4] (ii) hydrate nucleation at the water-oil interface,[5] followed by the growth of hydrate shells around a water core;[6] (iii) agglomeration between hydrate particles,[7] which increases the viscosity of the hydrate slurry;[8] and (iv) jamming of slowly-moving aggregates.[9] Figure 1 provides an illustration of this process, which highlights the cohesive interaction between hydrate particles.

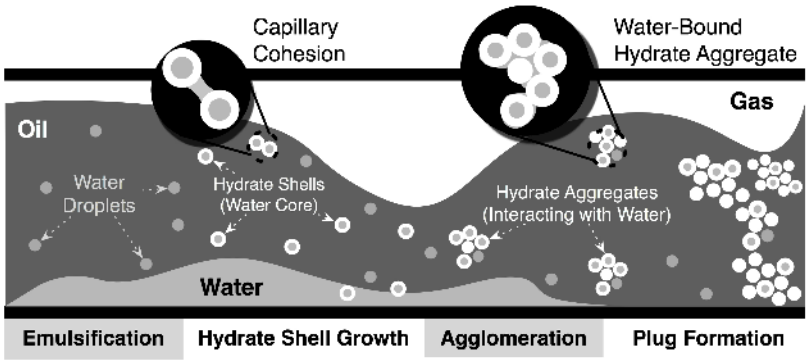

Figure 1. Hydrate plug formation mechanism for oil-dominant systems proposed by Turner et al.[3] in collaboration with J. Abrahamson (U. Canterbury).

To date, three classes of inhibitor have been developed to control hydrate plug formation. First, thermodynamic inhibitors (THIs) function to shift the hydrate equilibrium curve toward higher pressure and lower temperature conditions.[10] Despite their current prevalence in the industry, the amount of THI required to fully prevent hydrate formation in some deep-water flowlines may be cost-prohibitive. To maintain economic viability in deep water, kinetic hydrate inhibitors (KHIs) were developed to prevent the formation of hydrate blockages at low dosage rates,[11] which function by adsorbing to the interface of growing hydrate crystals to inhibit the continued assembly of cages.[12] Kinetic hydrate inhibitors provide a partial hydrate solution, as their performance may be weakened if the subcooling from hydrate equilibrium exceeds 10 K.[13] Fundamentally, both THIs and KHIs operate on the principle that hydrate risk is mitigated or managed by preventing hydrate formation in the first place. In the past decade, hydrate anti-agglomerants (AAs) have been developed to control hydrate plugging risk by minimizing particle cohesion and agglomeration potential. Huo et al.[14] proposed that surfactants – particularly quaternary ammonium salts[15] – mixed with the oil phase may weaken the capillary water bridge formed between hydrate particles.[16] Laboratory and field tests have shown AA performance may be satisfactory in oil-continuous systems with watercut conditions below 50 vol%;[17] the improvement of AA performance at high watercut[18] and in gas-dominant systems remains an area for future development. Anti-agglomerants provide an attractive platform for technology development, because they operate independent of pipeline length. However, as some of the AA chemical structures reported in the literature may conflict with regional environmental regulations, the use of these chemicals may be limited by overboard water quality.[19]

Recent studies have focused on the ability for some crude oils to naturally stabilize water-in-oil emulsions, where naturally-occurring surface active asphaltene components[20] and/or naphthenic acids[21] adsorb to and stabilize the water-oil interface. The nonionic hydrophilic groups in these surfactants may not adsorb as strongly to the water-oil interface as the ionic surfactants that are commonly found in anti-agglomerants,[13] but in large quantities these natural surfactants may fully stabilize hydrate-in-oil dispersions. As such, there is a strong economic incentive to develop laboratory-based techniques that can quantify the inherent hydrate-in-oil dispersion stability.

The current generation of laboratory techniques for such studies typically form hydrate by pressurizing water-in-oil emulsions at a low-temperature condition, where the emulsion is produced using deionized water. The use of deionized water was traditionally justified by the need to maintain a well-characterized hydrate equilibrium condition, as salt ions have a THI effect that increases with their concentration in the aqueous phase.[1] However, recent results have demonstrated an increase in water-in-oil emulsion stability when salt ions are present,[22] suggesting that such ions may increase the adsorption density of nonionic surfactants[23] to further reduce water-oil interfacial tension. In cases where ionic surfactants are present in the system, the use of deionized water may be offset in part by the presence of the surfactants' counter ions. Studies using a high-pressure automated lag-time apparatus[24] have demonstrated that both salt ions[25] and surfactants[26] may suppress the probability of nucleating gas hydrate for a given subcooling condition. While salt is well known for its THI properties, highly saline systems will also lower the driving force for nucleation and growth of the hydrate phase, because they reduce the equilibrium solubility of hydrocarbon components in the aqueous phase.[25] Understanding and

incorporating salt-induced changes to gas solubility into kinetic growth models is an important area for future work. In the present study, however, hydrates were intentionally formed under high (50 K) subcooling conditions, so that the effect of brine concentration on growth kinetics was negligible. Moreover, the focus of these experiments was not hydrate growth, but rather to improve the limited current understanding as to whether the addition of salt ions – which may increase the effectiveness of natural surfactants in the oil – can enhance the stability of hydrate-in-oil dispersions. This study seeks to quantify the stability of hydrate-in-oil dispersions with varying salt concentrations in the aqueous phase, to determine whether brine salinity should be considered in future investigations of hydrate-in-oil dispersion stability.

2 EXPERIMENTAL METHODS

2.1 Emulsion Preparation

This study employed the same Australian crude oil that was previously used by Aman et al.,[27] with density and viscosity of 0.85 g/ml and 4.7 cP, respectively, at 20 °C and 1 bar. Water-in-oil emulsions were prepared with 30 vol% brine added drop-wise into the crude oil while being homogenized at 17,800 RPM for 180 seconds.[28] The emulsions were ripened for 24 hours prior to use. Through bottle stability tests, the emulsions formed with deionized water and this crude oil were found to be macroscopically stable for at least 7 days (i.e. no clarified water phase was observed). The emulsions were stored away from sunlight at 20 °C and emulsion samples were drawn with a pipette.

The interfacial tension (IFT) between the crude oil and water at varying salinity was measured using a pendant drop method[29] with a Theta Lite optical tensiometer from OneAttension

instruments. Crude oil droplets were generated in the brine phase for optical clarity, and were monitored up to 10,000 s to ensure the measurement had reached steady-state. A first set of tests was performed with crude oil droplets and an aqueous phase of 0-10 wt% NaCl. In a second set of tests, the crude oil was first mixed with chemically inert paraffin oil (0-100 wt%) to qualitatively assess the effectiveness of the natural surfactants in the crude oil.

2.2 Differential Scanning Calorimeter

Hydrate-in-oil dispersion stability was evaluated using a three-cell Differential Scanning Calorimeter (DSC) from Calorimetry Sciences Corporation (now TA instruments). The DSC contained a reference cell (Figure 2), which enabled a differential measure of the heat flows into the three experiment cells to be measured. Resistance thermometers were used to monitor the cell temperature. The DSC achieved the target temperature by adding or removing heat from each experimental cell through an array of Peltier modules. Each cell was connected to a high-pressure manifold rated to 14.0 MPa and supplied with ultra-high purity methane using a regulator. The uncertainties in the temperature and integrated heat flux measurements for this DSC were estimated to be ±0.5 °C and ±4%, respectively, by Hughes.[30]

In each experiment, approximately 10-30 mg of water-in-oil emulsion was pipetted into each of the experimental cells, and the gas phase was replaced (by flushing) with ultra-high purity methane (>99.999%) at 6.2 MPa and 15 °C. The cells were isolated from the manifold, and the DSC temperature control program was engaged to conduct a repetitive four-step cycle as used by Aman et al.:[27] (i) cooling from 20 to -30 °C at a rate of 0.9 °C/min; (ii) one-hour hold at -30 °C to allow for complete hydrate conversion; (iii) heating from -30 to 0 °C at a rate of 0.9 °C/min; and (iv) heating from 0 to 15 °C at a rate of 0.07 °C/min to increase heat flow resolution during methane hydrate dissociation. During the first temperature cycle, the crude oil was partially

saturated with methane and, in addition, a small quantity of ice was detected by an endothermic peak at 0 °C. The formation of ice in the first cycle was caused by the limited saturation of methane in the liquid hydrocarbon phase, which meant that some of the water droplets could not be converted to hydrate on the cooling and heating timescale described above. After the first temperature cycle, no ice peaks were detected during heating.

The integrated area of the DSC thermogram measured during heating step (iv) corresponded directly, via the enthalpy of hydrate formation, to the amount of hydrate dissociated in the trial. In the case that the hydrate dispersion was unstable, the integrated area was observed to decrease with each hydrate formation-dissociation cycle. When hydrate particles were dissociated, both water and gas were generated, the latter of which was highly buoyant within the crude oil phase. As gas bubbles rose in an unstable dispersion, they generated local turbulence that was sufficient to enable coalesce of nearby water droplets; this coalescence increased the diameter of water droplets. Recent studies have measured hydrate shell thickness to be consistently below 50 microns within 24 hours of nucleation;[31] diffusion limitations through the hydrate shell restrict the hydrate growth rates by multiple orders of magnitude[3] after the initial shell growth. As water droplet diameters grew beyond 100 microns, the total surface area available for hydrate shell growth decreased; the amount of hydrate formed when the system was next cooled below the hydrate equilibrium condition decreased as a consequence of the reduced interfacial area. This process is illustrated in Figure 2, where the volume of hydrate in each formation-dissociation cycle decreases if droplets coalesce in the unstable dispersion.

The stability of hydrate-in-oil dispersions may be sensitive to the amount of surfactant that is adsorbed to the hydrate-oil interface.[32] If strong surfactants have absorbed to the hydrate interface prior to dissociation, the local turbulence generated by rising gas bubbles may mitigate the coalescence of the water droplets.

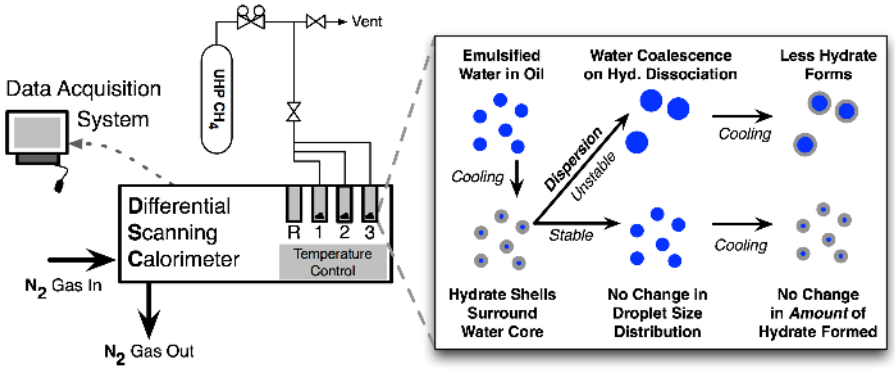

Figure 2. Schematic of high-pressure differential scanning calorimeter and procedure employed in this study.

In DSC experiments, ten hydrate formation-dissociation cycles were conducted for emulsions where the aqueous phase was comprised of deionized water mixed with between 0 and 10 wt% NaCl. As mentioned above, limited methane saturation of the liquid hydrocarbon phase in the first cooling cycle resulted in a limited amount of hydrate formation. In all trials, the largest volume of hydrate formed in the second temperature cycle. That is, emulsified droplets were unable to convert to hydrate if the oil phase was not fully saturated with methane. In unstable hydrate-in-oil dispersions, the amount of hydrate formation detected in the second through tenth trials decreased to varying extents, as discussed below.

2.3 Nuclear Magnetic Resonance (NMR) Emulsion Characterization

Stejskal and Tanner first demonstrated how the measurement of molecular self-diffusion in liquid can be performed via NMR pulsed field gradient (PFG) methods.[33] These measure NMR signal attenuation due to the random motion (diffusion) of the relevant molecules during the time between the sequential application of magnetic field gradients across the sample. The resultant NMR signal loss (S/S_0) is quantified as:

$$\ln\left(\frac{S}{S_0}\right) = exp\left(-\underline{D}(\gamma\delta g)^2\left(\Delta - \frac{\delta}{3}\right)\right), \quad (1)$$

where $\underline{D}$ is the self-diffusion coefficient of the molecules, Δ is the temporal duration between application of the sequential magnetic field gradients, δ is the duration of the magnetic field gradient, g is the strength of the magnetic field and γ is the gyro-magnetic ratio of the ^1H nucleus as used here ($\gamma = 2.68\times10^8\ T^{-1}s^{-1}$). The signal S is thus measured as a function of g, δ or occasionally Δ enabling the extraction of $\underline{D}$ via application of Eq. 1. The NMR pulse sequence frequently employed to achieve this is based on a stimulated spin echo.[34]

In the case of water in oil emulsions, the water molecules are contained within the droplet, meaning that diffusion of the water molecules is restricted. In this case, the NMR signal attenuation ($I=S(g)/S(g=0)$) can be approximated as:[35]

$$ln\, I\,(D,a,g,\delta) = -2\gamma^2 g^2 \sum_{m=1}^{\infty} \frac{1}{\alpha_m^2(\alpha_m^2 a^2 - 2)}\left[\frac{2\delta}{\alpha_m^2 D} - \frac{\psi}{(\alpha_m^2 D)^2}\right] \quad (2a)$$

$$\psi = 2 + exp^{-\alpha_m^2 D(\Delta-\delta)} - 2exp^{-\alpha_m^2 D\Delta} - 2exp^{-\alpha_m^2 D\delta} + exp^{-\alpha_m^2 D(\Delta+\delta)} \quad (2b)$$

where a is the droplet radius, α_m is the m^{th} positive root of the equation:

$$J_{5/2}(\alpha\alpha) - \frac{1}{\alpha\alpha} J_{3/2}(\alpha\alpha) = 0 \qquad (2c)$$

and where J_k is the Bessel function of the first kind of order k. Eq. 2 assumes a Gaussian shape for the NMR signal phase distribution (known as the Gaussian phase distribution (gpd) model). An alternative to Eq.2 also exists in which it is assumed that the duration of the applied magnetic field gradient, δ, is zero (known as the short gradient pulse (sgp) approximation) (e.g. Grebenkov [36]). Lingwood et al.[37] demonstrated for the case of restricted diffusion inside spherical droplets, that the block gradient pulse (bgp) approximation method is more accurate than either the Gaussian phase distribution (gpd) assumption or the short gradient pulse (sgp) approximation. This bgp method is based on a generalized gradient waveform set of methods,[38] in which the Bloch-Torrey equation is solved by eigenfunction expansion in the presence of a piecewise-constant gradient waveform.[39] Details regarding the derivation can be found in Grebenkov[40] and details regarding the implementation of this method for emulsion droplet sizing, as is employed in this work, can be found in Lingwood et al.[37]

Equation 2 and the bgp method are valid only for an emulsion with a single droplet size. In reality most emulsions are a distribution of droplet radii, $P(a)$, meaning that the measured signal is given by:

$$I(D, g, \delta) = \frac{\int_0^\infty a^3 P(a) I(D, a, g, \delta) da}{\int_0^\infty a^3 P(a) da} \qquad (3)$$

where $I(D,a,g,\delta)$ is the signal attenuation function described above in Eq.2.

The extraction of $P(a)$ from Eq. 3, which is the number based distribution of emulsion droplet radii, is both an ill-conditioned matrix inversion (when tackled analytically) and an unstable minimization problem (when tackled numerically). Progress can be made if an assumption about

the droplet size distribution shape is made: typically a log-normal distribution is assumed. However, Hollingsworth et al.[41] demonstrated that the use of Tikinov regularisation to numerically invert Eq. 3 with the Generalised Cross Validation (GCV) technique used to select the regularization parameter does not require any assumption regarding the droplet size distribution shape in order to render it numerically stable.

Johns et al.[42] have demonstrated the ability of low-field NMR methods to accurately capture water-in-oil droplet size distributions (DSDs) based on restricted diffusion measurements employing pulsed field gradient (PFG) techniques. When compared to visual microscopy, NMR is able to sample the whole sample and can be readily applied to opaque and concentrated emulsion samples. In this study, an ACT-Aachen (now Magritek) 1 T Halbach Array permanent magnet and accompanying spectrometer, featuring a 1 T/m magnetic field gradient, was used to measure the DSD for the water-in-oil emulsions detailed in Section 3.1. The ^{1}H signal was detected at a resonance frequency of 43.36 MHz. The magnet provided sufficient homogeneity such that chemical shift spectral differences could be used to unambiguously distinguish between the signals from the water and oil phases as demonstrated previously.[43]

Emulsions were sampled at 24-hour intervals after creation and placed in 5 mm outer-diameter sample tubes that could be accommodated within the magnet array. The magnet operates optimally at 27 °C and so this was the temperature at which the NMR experiments were performed. Droplet size measurements were acquired using a pulsed field gradient stimulated spin echo (PFG SSE) sequence; the maximum gradient strength used was 1 T/m, with a 4 ms gradient pulse duration (δ) and a 350 ms observation time (Δ); 32 repeat scans were performed

with 16 gradient increments from 0 T/m to the 1 T/m maximum gradient strength. NMR signal intensities were transformed into DSDs by Tikhonov regularization.[42a] In each experiment, emulsions were characterized as stable if the number mean droplet size was not observed to increase by more than 1 micron over a four day observation window.

3 RESULTS AND DISCUSSION

3.1 DSC Results for Saline Hydrate-in-Oil Dispersions

The addition of 10 wt% NaCl decreased the hydrate equilibrium temperature to about 3 °C from the value of about 9 °C observed for the experiments with DI water. This shift of 6 °C is consistent with predictions of the change in methane hydrate equilibrium temperature caused by the addition of 10 wt% NaCl. The methane hydrate equilibrium temperature at 60 bar is predicted by Multiflash 4.1 with the CPA-Infochem model set[44] to be 8.2 °C for pure water and 3.5 °C for a system containing 10 wt% NaCl. In both cases, the maximum heat flow (Figure 3) occurred at a higher temperature than the equilibrium value predicted by Multiflash, which may be due to the time lag introduced by heating through the hydrate equilibrium boundary within approximately 30 minutes. The thermograms (Figure 3) for the 10 wt% NaCl samples had a different baseline to those obtained with DI water during the period of hydrate dissociation, because the hydrate equilibrium condition was closer to the temperature (0 °C) at which the DSC heating rate was changed as per Section 2.2. The addition of 10 wt% NaCl to the aqueous phase produced minimal change in the integrated area of the DSC thermograms over 10 hydrate formation-dissociation trials, indicating that the dispersion was stable. In contrast the dispersion

formed with the 0 wt% NaCl in the aqueous phase showed a monotonic decrease in the integrated area over cycles 2 to 10, with a final area about 20 % of that in Cycle 2.

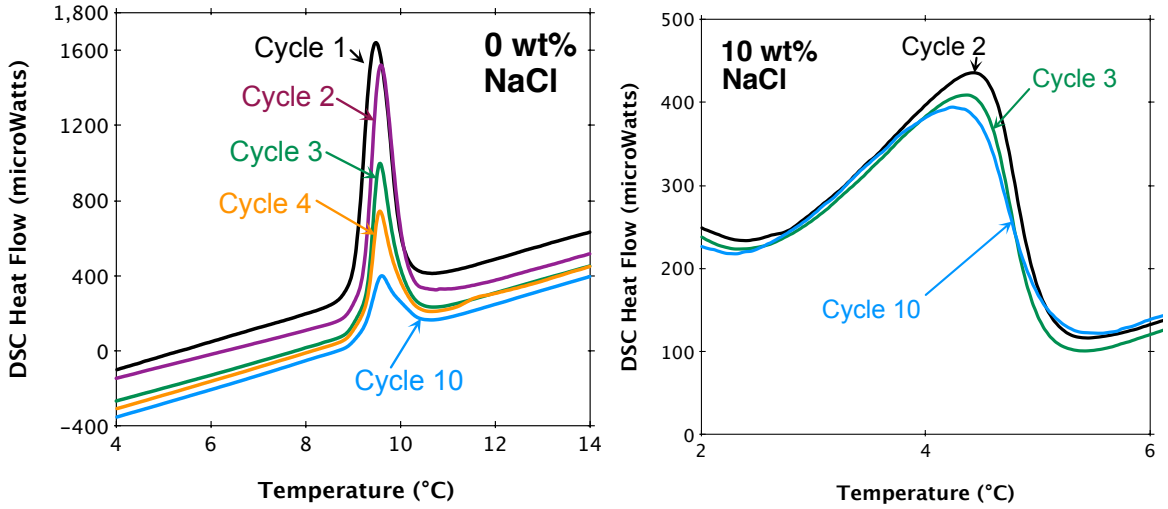

Figure 3. Example DSC thermograms for methane hydrate-in-oil dispersions dissociating at approximately 1000 psi with (left) 0 wt% and (right) 10 wt% NaCl in the aqueous phase. The temperature scan rate in each case was 0.07 °C/min; the integrated area under each peak is proportional to the amount of hydrate present in each temperature cycle.

For systems with 0-10 wt% NaCl, the integrated heat flow from each cycle was normalized to the integrated heat flow of cycle 2 (Figure 4) to quantify the hydrate-in-oil dispersion stability in each cycle. In the context of this work, the use of the term "stability" refers to a non-aggregating or non-coalescing dispersion of hydrate or water, respectively, in the oil phase; hydrate was thermodynamically stable in each of the trials shown in Figure 4, as evidenced by the measureable heat flow over hydrate dissociation shown in Figure 3. Unstable dispersions were characterized by a decrease in the relative integrated heat flow *below* 80% of the first trial, which was established by Aman et al.[27] as the repeatability boundary for this DSC method. That is,

values of the integrated heat flow which deviate below the shaded region in Figure 4 correspond to cases where the dispersion becomes unambiguously less stable with continued hydrate formation and dissociation cycles. The asymptotic behavior with increasing cycle number shown in Figure 4 may correspond to the coalescence of water droplets to form a free water phase, for which the water-oil interfacial area will change negligibly during hydrate dissociation. The results shown in Figure 4 clearly demonstrate that, for the crude oil used in this investigation, the addition of salt ions increases the hydrate-in-oil dispersion stability. Within the 20% uncertainty in the measurement,[27] the hydrate-in-oil dispersions formed with at least 5 wt% NaCl in the aqueous phase could be characterized as stable (Figure 4). The degree of stability is similar to that obtained previously by Aman et al.[27] for systems containing an ionic surfactant at concentrations of around 0.1 wt % in the crude oil phase.

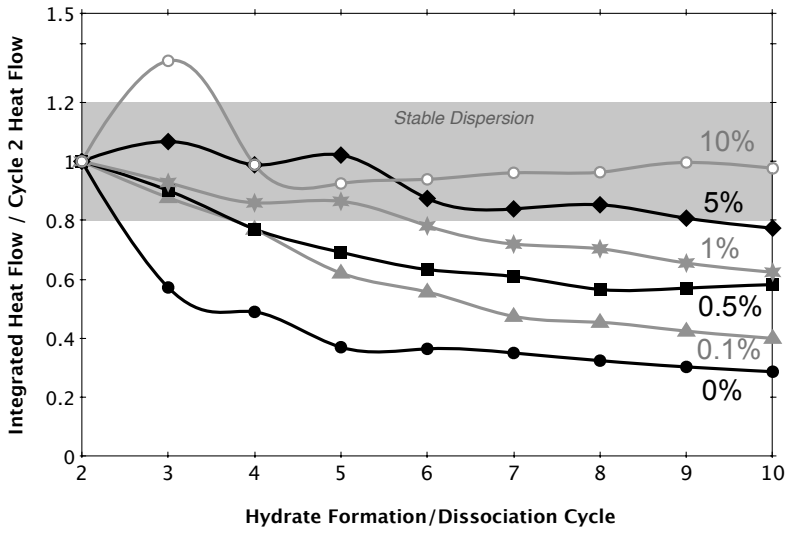

Figure 4. Integrated heat flow in DSC as a function of hydrate formation/dissociation cycle, for each salt concentration.

3.2 Comparison Between Nonionic and Ionic Surfactant-Stabilized Dispersions

Previous hydrate-in-oil dispersion stability studies using a DSC successfully demonstrated that the addition of centrylpyridium chloride (CPC, an ionic surfactant) generated a step-change in dispersion stability at mass fractions above 3×10^{-6}.[27] Hydrate-in-oil stability data for both CPC and brine systems are shown in Figure 5, which demonstrates that the addition of at least 5 wt% NaCl generated a stable dispersion, comparable to the performance of an ionic surfactant at high concentration (2 wt%). The step-change in stability observed for the CPC system (Figure 5) corresponds to the onset of strong surfactant adsorption at the hydrate-oil interface. This step change in stability is not observed in the saline systems, which suggests that the salt ions may function solely to increase the hydrophilicity of nonionic surfactants in the crude oil phase. Interfacial tension (IFT) measurements between water and oil were used to compare the hydrophilicity of CPC with the crude oil's nonionic surfactants. In the case of CPC, it is unlikely that the chloride counter-ion provides a measureable improvement to dispersion stability, as the NaCl mass fractions required to stabilize the dispersion were 100 times higher than that measured for stabilization by CPC (Figure 5).

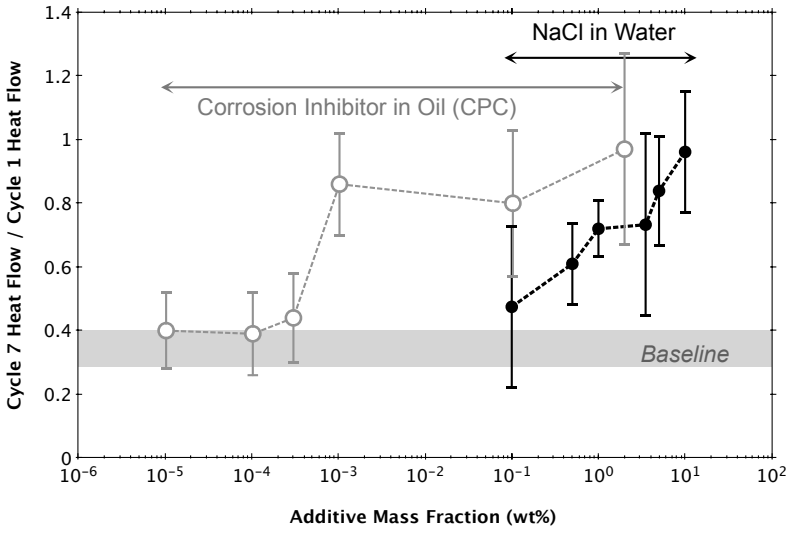

Figure 5. Average integrated heat flow on the seventh hydrate formation/dissociation cycle, for systems containing corrosion inhibitor (CPC) in the oil phase (grey open points) and salt in the water phase (closed black points). Error bounds correspond to a 95% confidence interval across six independent repeat trials.

The IFT was measured between water and paraffin oil, where the oil phase contained between 0.001 and 100 wt% of the crude oil discussed above. The results (Figure 6) show a decrease in water-oil IFT with crude oil fraction, with a minimum IFT (18.7±0.2 mN/m) measured at 100 wt% crude oil with deionized water. The trend of decreasing IFT with crude oil fraction in Figure 6 suggests that natural surfactants in the crude oil adsorbed to the water-oil interface; the IFT did not reach a plateau below 100 wt% crude oil, suggesting the water-oil interface was not saturated with surfactant. The addition of both 5 and 10 wt% NaCl to the aqueous phase decreased the IFT from the baseline with deionized water. For the example of a pure crude oil system with 10 wt% NaCl, the steady-state IFT (12.8±0.6 mN/m) agreed well with the IFT generated with 2 wt% CPC in the oil phase (11.9±0.6 mN/m). The agreement between IFT values for systems with (i) 10 wt% NaCl and (ii) 2 wt% CPC suggests that the addition of ions to the aqueous phase increases the hydrophilicity of the natural surfactants in this crude oil, and may allow them to adsorb at the water-oil interface with comparable effectiveness to the ionic surfactant.

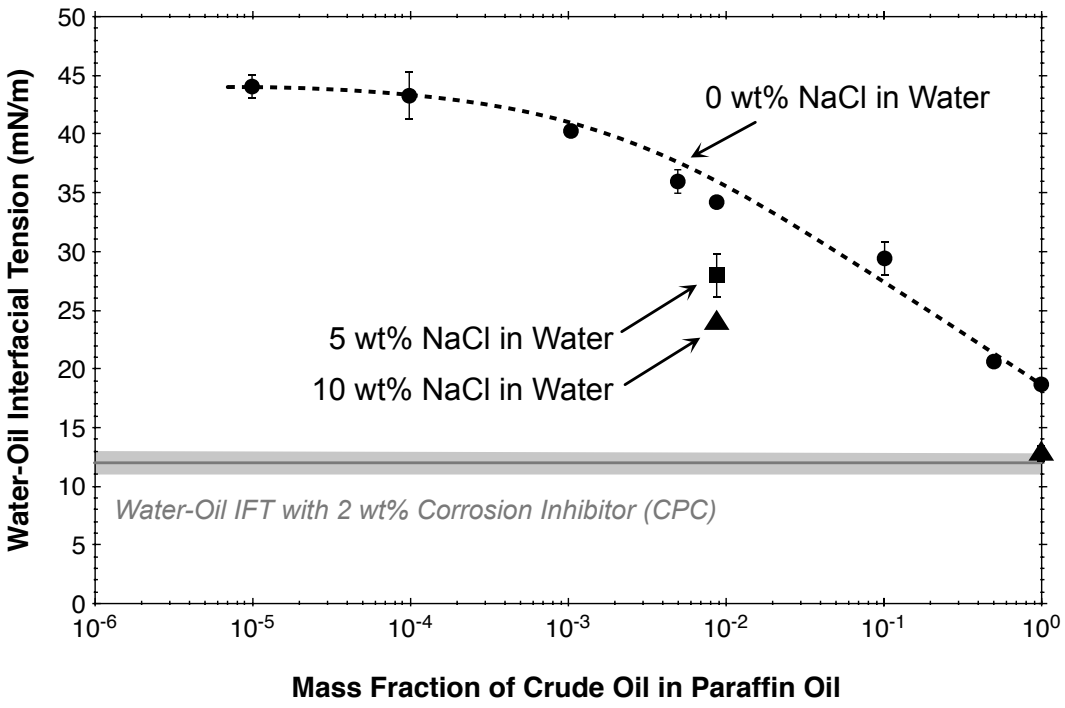

Figure 6. Water-oil interfacial tension with 0, 5 and 10 wt% NaCl in the aqueous phase, compared to the equilibrium value obtained for a system with 2 wt% corrosion inhibitor in the paraffin oil phase.

Previous DSC dispersion stability studies have suggested that surfactants (either ionic or nonionic) prevent droplet coalescence by adsorbing to the hydrate-oil interface, where hydrate-in-oil dispersions were stabilized at surfactant concentrations up to 100 times below the critical micelle concentration observed for the water-oil interface.[27] However, the results in Figure 6 suggest that the addition of salt in the aqueous phase would likely enhance the water-in-oil emulsion stability. To establish whether the stabilizing trend observed in saline DSC thermograms (Figure 3) corresponded to changes in the hydrate-oil or water-oil interface, the water-in-oil emulsion stability was measured directly via NMR using the procedure discussed above.

3.3 Comparative Effect of Brine Salinity on Water-Oil Emulsion Stability

While increasing the aqueous phase NaCl fraction could provide a strong benefit in terms of hydrate dispersion stability and, consequently, the stabilized transport of a hydrate-laden slurry in the flowline, the impact of brine salinity on water-in-oil emulsion stability is also critical in the design and management of subsea oil and gas systems. First, emulsions that are stable for at least 24 hours during shut-in (non-flowing) conditions decrease the risk of forming a hydrate blockage on restart; the coalescence of water droplets into a free water phase may result in the formation of a cold gas bubble-in-water dispersion on restart, which has been reported to correspond to a catastrophic risk of hydrate blockage.[45] Second, if emulsions are stable for longer periods of time (e.g. 96 hours) under quiescent conditions, additional energy and cost may be required to break the emulsion at the receiving facility.

The water-in-oil emulsion stability was studied over several days with low-field NMR measurements, where 0 to 10 wt% NaCl was added to the brine phase according to the procedure in Section 2.3. The results show that increasing the NaCl fraction in water did not change the shape of the DSD measured 24 hours after preparation (right panel of Figure 7), but functioned to decrease the mean droplet radius by more than 50% at high brine concentrations. As the mixing energy used to generate each emulsion was comparable (Section 2.1), this result is qualitatively consistent with the water-oil IFT measurements discussed above.

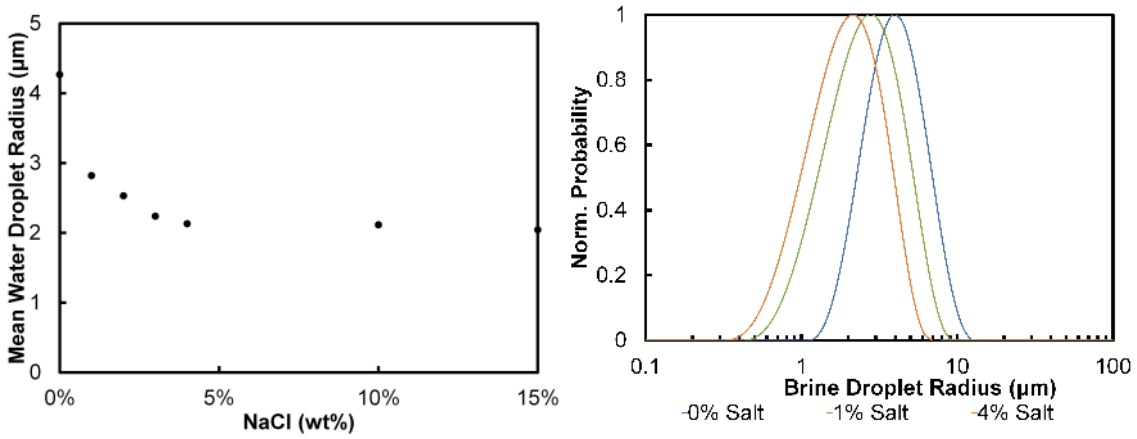

Figure 7. Water-in-oil droplet radius measured via low-field NMR measured 24 hours after emulsions were created: (left) mean values for 0-10 wt% NaCl in water; and (right) DSDs for 0, 1, and 4 wt% NaCl in water.

Each water-in-oil emulsion with 0-10 wt% NaCl was monitored in the low-field NMR on a 24-hour basis, to quantify the emulsion stability. At 0 wt% NaCl, the mean water droplet radius increased linearly by a factor of three over a 96-hour observation period (Figure 8). At 0.1 wt% NaCl in the aqueous phase, no change was observed in the mean droplet size over 96 hours, which suggests that only a mild degree of brine salinity is required to stabilize the water-in-oil emulsion at 30% watercut. Systems with higher mass fractions of NaCl showed similar behavior, and were excluded from Figure 8 for clarity.

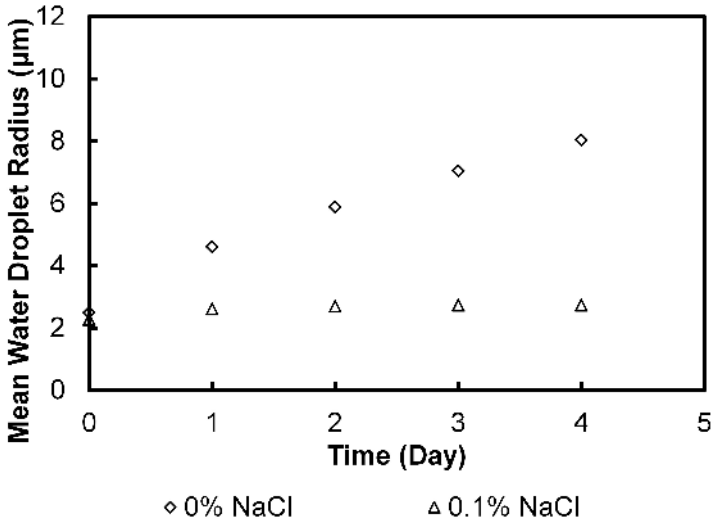

Figure 8. Mean water droplet radius as a function of time after the water-in-oil emulsion was generated; the droplet radius increased linearly for the system with deionized water, while no significant change was detected for systems with at least 0.1 wt% NaCl in the aqueous phase.

Together, the results suggest that – for the crude oil studied here – brine salinity strongly increases both hydrate-in-oil dispersion stability and water-in-oil emulsion stability. The NMR data demonstrate that only 0.1 wt% NaCl was required to stabilize the water-in-oil emulsion (Figure 8), while at least 5 wt% NaCl was required to stabilize the DSC thermogram (Figure 4); this comparison suggests that the integrated DSC thermogram corresponds to a measurement of hydrate-in-oil dispersion stability. For the emulsion system, no *adverse* consequence was observed on emulsion stability when the NaCl concentration was increased above 0.1 wt%, although higher mass fractions (5-10 wt%) were observed to decrease the average droplet diameter; additional studies would be required to determine whether these mild decreases in droplet size would likely impact on the cost of emulsion breaking at the receiving facility. However, any assessment of cost should also consider the potential savings associated with the

significant increases in hydrate-in-oil dispersion stability observed for NaCl mass fractions above 5 wt%, which had a stability comparable to a system containing 2 wt% ionic surfactant (similar to a hydrate anti-agglomerant, or AA). This result suggests that highly saline systems may provide a natural AA-type behavior in flow, depending on the natural surfactant distribution in the oil phase. Of course, the DSC experiments in this study were conducted under shear-free conditions and the ultimate test of AA-type inhibition performance should involve levels of shear approaching those found in a production pipeline. To further investigate the AA inhibition performance of saline systems in a given crude oil, tests with laboratory-scale shear equipment should be conducted, which represents an ongoing area of work.

4 Conclusions

Hydrate-in-oil dispersion stability was studied using a DSC, where methane hydrate was formed from water-in-crude oil emulsions containing 0-10 wt% NaCl in the aqueous phase. A monotonic increase in hydrate dispersion stability was observed with increasing brine salinity. Dispersions formed with at least 5 wt% NaCl in the aqueous phase were found to be have the same stability as systems studied previously with 2 wt% ionic surfactant in the oil phase. Water-in-crude oil emulsion stability was quantified using a low-field NMR apparatus, where the addition of at least 0.1 wt% NaCl resulted in an unchanging droplet radius over the 96-hour observation window. The results together demonstrate that increasing brine salinity may increase the activity of natural surfactants in the crude oil phase. Depending on the distribution of natural surfactants, highly saline systems may therefore behave similarly to those containing hydrate anti-agglomerants, decreasing both the risk of severe hydrate blockage and the necessity of

costly hydrate inhibition. This result suggests that hydrate-laden slurries made with deionized water may show reduced aggregation and improved transport behavior, where the consideration of realistic brine salinity may be critical to capturing reliably the stability of emulsions and dispersions in the flowline.

Acknowledgements

This work was funded in part by the Australian Research Council through LE110100189 and DP130101461. ZMA acknowledges the University of Western Australia for a Research Development Award. EFM acknowledges Chevron for their support of the research through the Gas Process Engineering endowment. The authors thank Ken Marsh for the donation of the DSC.

References

1. Sloan, E. D.; Koh, C. A., *Clathrate Hydrates of Natural Gases*. Third Edition ed.; CRC Press, Taylor & Francis Group: Boca Raton, FL, 2007.
2. Kelkar, S. K.; Selim, M. S.; Sloan, E. D., Hydrate dissociation rates in pipelines. *Fluid Phase Equilibria* **1998,** *150-151*, 371-382.
3. Turner, D.; Miller, K.; Sloan, E., Methane hydrate formation and an inward growing shell model in water-in-oil dispersions. *Chemical Engineering Science* **2009,** *64*, 3996-4004.
4. Boxall, J. A.; Koh, C. A.; Sloan, E. D.; Sum, A. K.; Wu, D. T., Droplet Size Scaling of Water-in-Oil Emulsions under Turbulent Flow. *Langmuir* **2012,** *28* (1), 104-110.
5. Walsh, M. R.; Koh, C. A.; Sloan, E. D.; Sum, A. K.; Wu, D. T., Microsecond Simulations of Spontaneous Methane Hydrate Nucleation and Growth. *Science* **2009,** *326* (5956), 1095-1098.
6. Taylor, C. J.; Miller, K. T.; Koh, C. A.; Sloan Jr., E. D., Macroscopic investigation of hydrate film growth at the hydrocarbon/water interface. *Chemical Engineering Science* **2007,** *62* (23), 6524-6533.
7. Aman, Z. M.; Brown, E. P.; Sloan, E. D.; Sum, A. K.; Koh, C. A., Interfacial mechanisms governing cyclopentane clathrate hydrate adhesion/cohesion. *Physical Chemistry Chemical Physics* **2011,** (13), 19796-19806.
8. Sinquin, A.; Palermo, T.; Peysson, Y., Rheological and Flow Properties of Gas Hydrate Suspensions. *Oil & Gas Science and Technology* **2004,** *59* (1), 41-57.

9. Lafond, P. G.; Gilmer, M. W.; Koh, C. A.; Sloan, E. D.; Wu, D. T.; Sum, A. K., Orifice jamming of fluid-driven granular flow. *Phys. Rev. E* **2013,** *87* (4), 8.
10. Sloan, E. D.; Koh, C. A.; Sum, A. K., *Natural Gas Hydrates in Flow Assurance*. Gulf Professional Publishing, Elsevier Inc.: 2011.
11. Sloan, E. D.; Subramanian, S.; Matthews, P. N.; Lederhos, J. P.; Khokhar, A. A., Quantifying Hydrate Formation and Kinetic Inhibition. *Ind. Eng. Chem. Res* **1998,** *37*, 3124-3132.
12. Carver, T.; Drew, M.; Rodger, P., Inhibition of Crystal Growth in Methane Hydrate. *J. Chem. Soc. Faraday Trans.* **1995,** *91*, 3449-3460.
13. Kelland, M., History of the Development of Low Dosage Hydrate Inhibitors. *Energy & Fuels* **2006,** *20* (3), 825-847.
14. Huo, Z.; Freer, E.; Lamar, M.; Sannigrahi, B.; Knauss, D.; Sloan, E. D., Hydrate plug prevention by anti-agglomeration. *Chemical Engineering Science* **2001,** *56*, 4979-4991.
15. Zanota, M.; Dicharry, C.; Graciaa, A., Hydrate Plug Prevention by Quarternary Ammonium Salts. *Energy & Fuels* **2005,** *19* (2), 584-590.
16. Yang, S.-o.; Kleehammer, D.; Huo, Z.; Sloan, J., E Dendy; Miller, K., Temperature dependence of particle-particle adherence forces in ice and clathrate hydrates. *Journal of Colloid and Interface Science* **2004,** *277*, 335-341.
17. Gao, S., Hydrate Risk Management at High Watercuts with Anti-agglomerant Hydrate Inhibitors. *Energy & Fuels* **2009,** *23*, 2118-2121.
18. Sun, M.; Firoozabadi, A., New Hydrate Anti-Agglomerant Formulation for Offshore Flow Assurance and Oil Capture. In *SPE Offshore Technology Conference*, 2014.
19. Webber, P., Fundamental Understanding on the Effects of Anti-Agglomerants Toward Overboard Water Quality. In *SPE Offshore Technology Conference*, 2010.
20. Schorling, P.; Kessel, D.; Rahimian, I., Influence of the crude oil resin/asphaltene ratio on the stability of oil/water emulsions. *Colloids and Surfaces A: Physicochemical and Engineering Aspects* **1999,** *152*, 95-102.
21. (a) Meredith, W.; Kelland, S.-J.; Jones, D., Influence of biodegradation on crude oil acidity and carboxylic acid composition. *Organic Geochemistry* **2000,** *31*, 1059-1073; (b) Qian, K.; Robbins, W.; Hughey, C.; Cooper, H.; Rodgers, R.; Marshall, A., Resolution and Identification of Elemental Compositions for More than 3000 Crude Acids in Heavy Petroleum by Negative-Ion Microelectrospray High-Field Fourier Transform Ion Cyclotron Resonance Mass Spectrometry. *Energy & Fuels* **2001,** *15*, 1505-1511; (c) Rogers, V.; Liber, K.; MacKinnon, M., Isolation and characterization of naphthenic acids from Athabasca oil sands tailings pond water. *Chemosphere* **2002,** *48*, 519-527; (d) Clemente, J.; Fedorak, P., A review of the occurence, analyses, toxicity, and biodegradation of naphthenic acids. *Chemosphere* **2005,** *60*, 585-600.
22. Effect of calcium salts and surfactant concentration on the stability of water-in-oil (w/o) emulsions prepared with polyglycerol polyricinoleate. **2010,** *341* (1), 101-108.
23. Alberty, R., On the Derivation of the Gibbs Adsorption Equation. *Langmuir* **1995,** *11* (9), 3598-3600.
24. Wu, R.; Kozielski, K. A.; Hartley, P. G.; May, E. F.; Boxall, J.; Maeda, N., Probability distributions of gas hydrate formation. *AIChE Journal* **2013,** *In Press*.
25. Sowa, B.; Zhang, X. H.; Hartley, P. G.; Dunstan, D. E.; Kozielski, K. A.; Maeda, N., Formation of Ice, Tetrahydrofuran Hydrate, and Methane/Propane Mixed Gas Hydrates in Strong Monovalent Salt Solutions. *Energy & Fuels* **2014,** *28* (11), 6877-6888.

26. Sowa, B.; Maeda, N., Probability Distributions of Natural Gas Hydrate Formation in Sodium Dodecyl Sulfate Aqueous Solutions. *Energy & Fuels* **2015,** *29* (9), 5692-5700.
27. Aman, Z. M.; Pfeiffer, K.; Vogt, S. J.; Johns, M. L.; May, E. F., Corrosion inhibitor interaction at hydrate–oil interfaces from differential scanning calorimetry measurements. *Colloids and Surfaces A: Physicochemical and Engineering Aspects* **2014,** *448* (0), 81-87.
28. Lachance, J.; Sloan, E. D.; Koh, C. A., Effect of hydrate formation/dissociation on emulsion stability using DSC and visual techniques. *Chemical Engineering Science* **2008,** *63*, 3942-3947.
29. Lin, S.-Y.; McKeigue, K.; Maldarelli, C., Diffusion-Controlled Surfactant Adsorption Studied by Pendant Drop Digitization. *AIChE Journal* **1990,** *36* (12), 1-11.
30. Hughes, T. J. Plug Formation and Dissociation of Mixed Gas Hydrates and Methane Semi-Clathrate Hydrate Stability. University of Canterbury, 2008.
31. Haber, A.; Akhfash, M.; Loh, K.; Aman, Z. M.; Fridjonsson, E. O.; May, E. F.; Johns, M. L., Monitoring of Hydrate Shell Growth using NMR Techniques. *Langmuir* **2015,** *31* (32), 8786–8794.
32. Aman, Z. M.; Olcott, K.; Pfeiffer, K.; Sloan, E. D.; Sum, A. K.; Koh, C. A., Surfactant Adsorption and Interfacial Tension Investigations on Cyclopentane Hydrate. *Langmuir* **2013,** *29* (8), 2676-2682.
33. Stejskal, E. O.; Tanner, J. E., Spin Diffusion Measurements: Spin Echoes in the Presence of a Time-Dependent Field Gradient. *The Journal of Chemical Physics* **1965,** *42* (1), 288-292.
34. Johns, M. L.; Hollingsworth, K. G., Characterisation of emulsion systems using NMR and MRI. *Progress in Nuclear Magnetic Resonance Spectroscopy* **2007,** *50* (2-3), 51 - 70.
35. Murday., J. S.; Cotts, R. M., Self-Diffusion Coefficient of Liquid Lithium. *The Journal of Chemical Physics* **1968,** *48* (11), 4938-4945.
36. Grebenkov, D. S., Laplacian eigenfunctions in NMR. I. A numerical tool. *Concepts in Magnetic Resonance Part A* **2008,** *32A* (4), 277-301.
37. Lingwood, I. A.; Chandrasekera, T. C.; Kolz, J.; Fridjonsson, E. O.; Johns, M. L., Emulsion droplet sizing using low-field NMRwith chemical shift resolution and the block gradient pulse method. *Journal of Magnetic Resonance* **2012,** *214*, 281 - 288.
38. (a) Caprihan, A.; Wang, L. Z.; Fukushima, E., A Multiple-Narrow-Pulse Approximation for Restricted Diffusion in a Time-Varying Field Gradient. *Journal of Magnetic Resonance, Series A* **1996,** *118* (1), 94 - 102; (b) Callaghan, P. T., A Simple Matrix Formalism for Spin Echo Analysis of Restricted Diffusion under Generalized Gradient Waveforms. *Journal of Magnetic Resonance* **1997,** *129* (1), 74 - 84; (c) Ryland, B. N.; Callaghan, P. T., Spin Echo Analysis of Restricted Diffusion under Generalized Gradient Waveforms for Spherical Pores with Relaxivity and Interconnections. *Israel Journal of Chemistry* **2003,** *43* (1-2), 1-7.
39. Barzykin, A. V., Theory of Spin Echo in Restricted Geometries under a Step-wise Gradient Pulse Sequence. *Journal of Magnetic Resonance* **1999,** *139* (2), 342 - 353.
40. Grebenkov, D. S., NMR survey of reflected Brownian motion. *Rev. Mod. Phys.* **2007,** *79*, 1077-1137.
41. Hollingsworth, K. G.; Johns, M. L., Measurement of emulsion droplet sizes using PFG NMR and regularization methods. *Journal of Colloid and Interface Science* **2003,** *258* (2), 383 - 389.
42. (a) Johns, M. L.; Hollingsworth, K. G., Characterisation of emulsion systems using NMR and MRI. *Progress in NMR Spectroscopy* **2007,** *50* (2-3), 51-70; (b) Hollingsworth, K. G.; Johns, M. L., Measurement of emulsion droplet sizes using PFG NMR and regularisation methods.

Journal of Colloid and Interface Science **2003,** *258*, 383-389; (c) Johns, M. L., NMR studies of emulsion. *Current Opinion in Colloid & Interface Science* **2009,** *14* (3), 178-183.
43. Callaghan, P. T., *Principles of Nucleat Magnetic Resonance Microscopy*. First Edition ed.; Oxford University Press: USA, 1991.
44. Infochem *Multiflash for Windows 4.1*, Infochem Computer Services Ltd: London, 2012.
45. Joshi, S. V.; Grasso, G. A.; Lafond, P. G.; Rao, I.; Webb, E.; Zerpa, L. E.; Sloan, E. D.; Koh, C. A.; Sum, A. K., Experimental flowloop investigations of gas hydrate formation in high water cut systems. *Chemical Engineering Science* **2013,** *97*, 198–209.